

# Universality at integer quantum Hall transitions

Kun Yang, D. Shahar, R. N. Bhatt, D. C. Tsui and M. Shayegan

*Department of Electrical Engineering, Princeton University, Princeton, NJ 08544*

(February 1, 2008)

## Abstract

We report in this paper results of experimental and theoretical studies of transitions between different integer quantum Hall phases, as well as transition between the insulating phase and quantum Hall phases at high magnetic fields. We focus mainly on universal properties of the transitions. We demonstrate that properly defined conductivity tensor is universal at the transitions. We also present numerical results of a non-interacting electron model, which suggest that the Thouless conductance is universal at integer quantum Hall transitions, just like the conductivity tensor. Finite temperature and system size effects near the transition point are also studied.

71.30.+h, 73.40.Hm

## I. INTRODUCTION

Continuous (or second order) quantum phase transitions in many-electron systems are of general interest to condensed matter physicists.<sup>1</sup> Recently a class of such quantum phase transitions, namely the transitions between different quantum Hall plateaus, and the transition between a quantum Hall phase and an insulating phase at high magnetic field ( $B$ ), have been under extensive experimental<sup>2-14</sup> and theoretical<sup>15-37</sup> study. In the renormalization group (RG) language, continuous phase transitions are controlled by RG fixed points, and many properties of the transition depend only on which fixed point the transition is controlled by, or which universality class it belongs to, and independent of microscopic details of the system. The best known examples of such universal properties are of course the critical exponents. In principle, quantities that are dimensionless are possibly universal at the critical point. Of particular interest in the study of quantum Hall transitions is the conductivity tensor at the critical point, which in two dimensions (2D) can be expressed as dimensionless numbers times the fundamental unit of conductance,  $\frac{e^2}{h}$ . It has been suggested that they should be universal, both at superfluid-insulator transition,<sup>41</sup> and quantum Hall transitions.<sup>18</sup> In the latter case, which is the focus of the present paper, this suggestion has received support from both experimental<sup>11</sup> study at the quantum Hall-insulator transition at high magnetic field (or transition in the lowest Landau level), and numerical works in the lowest Landau level<sup>19</sup> and the network model.<sup>27,28</sup>

In this paper we will present further experimental evidence that supports the universality of conductivity tensor at integer quantum Hall transitions, in both the lowest Landau level and *higher* Landau levels; we also demonstrate that the transitions in different Landau levels are in the same universality class. We will also present results of numerical studies of the integer quantum Hall transitions, based on non-interacting electron models; our results suggest that another dimensionless quantity, the Thouless conductance, a quantity that is closely related to the longitudinal conductance of the system, is also universal at integer quantum Hall transitions.

By definition, a quantum critical point is a critical point at zero temperature ( $T = 0$ ). Real experiments, however, are always done at finite temperatures, and the critical point can only be reached asymptotically in the low temperature limit of the experiments. We will also present data on the  $T$  dependence of various physical quantities near the critical point, and study how the universal values of the resistivity (or conductivity) tensor are reached asymptotically. In a *noninteracting* system, the effect of a finite  $T$  is to set a finite dephasing length, which effectively divide an otherwise infinite system into incoherent finite pieces, and introduce finite size effects to the critical behavior. We have therefore also studied the size dependence of the Thouless conductance, near the critical point.

The paper is organized in the following way. In section II we present our experimental results on studies of the resistivity tensor, both at the high field QH-insulator *and* QH-QH critical points. We study their behavior not only in the asymptotic low temperature limit, but also the temperature dependence at higher temperature, and how the universal values are approached as temperature decreases. In section III we present results of our numerical study on a non-interacting electron model on a lattice, and demonstrate that at the critical points, the properly defined Thouless conductance is a universal number that is independent of the strength and type of random potential, amount of mixing between different Landau levels (subbands), whether there is particle-hole symmetry, etc. We also study the system size dependence of the Thouless conductance at the critical points, and demonstrate that the universal asymptotic value is reached at surprisingly small system sizes in the lowest Landau subband. In section IV we summarize our findings by discussing the relations between our experimental and numerical results, as well as their relevance to existing theoretical and experimental works on this subject.

## II. EXPERIMENTS

In this section we describe our experimental results. While our main finding has already been published before<sup>11</sup>, we will present here a more detailed account of our study of the QH

to Insulator at low  $T$ . Since the main motivation of our work was to test for the theoretically predicted *universal* features, we have set to study a broad range of samples that represents much of the available 2DES samples at the time of this work. In Fig. 1 we illustrate the large diversity of samples studied by plotting the mobility ( $\mu$ ) vs. density ( $n$ ) of some of our samples. The range of the axis in this figure is chosen to represent virtually the entire range of 2DES that is reported in the literature ( $\mu = 10^3 - 10^7$  cm<sup>2</sup>/Vsec and  $n = 10^9 - 10^{12}$  cm<sup>-2</sup>). As can be seen, our samples cover a significant area in of this log-log graph. To increase the generality of our results we obtained our samples from 6 different sources including 3 MBE, one LPE and two MO-CVD machines. To insure that geometrical factors, which are known to introduce modifications to transport in the QH regime, do not come into play in our study, we did not maintain a uniform sample geometry. Rather, our samples were cut in many different shapes: some where wet-etched in a Hall-bar shape of various dimensions, and others were cleaved in a square or rectangular shape with contacts diffused along the edges. The smallest contact to contact dimension was 100  $\mu$ m while the largest was 1 mm. Naturally, we did not adhere to a specific structure design of the wafers and there too diversity abound as we studied 2DES's embedded in GaAs/AlGaAs heterostructures and quantum wells (QW's), InGaAs/InAlAs QW's, InGaAs/InP heterostructures, AlAs/GaAs QW's, Ge/SiGe QW's and Si MOSFET's. The total number of samples studied at low  $T$ 's exceeds 150.

Quite generally, the QH series terminates, at high  $B$ , with a transition to an insulating phase. A typical transition is shown in Fig. 2, where we plot  $B$  traces of the diagonal resistivity,  $\rho_{xx}$ , taken at several  $T$ 's. The sample exhibit metallic behavior at low  $B$  followed by a set of integer QH states manifested by minima in  $\rho_{xx}$ . As  $B$  is further increased beyond  $\nu = 1$ ,  $\rho_{xx}$  increases for all  $T$ 's. If we examine, however, the  $T$  dependence of  $\rho_{xx}$  focusing on the high- $B$  region (Fig. 3), we observe a stark change in its character: In the QH region,  $\rho_{xx}$  increases with  $T$ , while at higher  $B$  the opposite occurs, and  $\rho_{xx}$  decreases with  $T$ . It is therefore reasonable to use the temperature coefficient of resistivity (TCR) to delineate two different transport regimes: The QH state (TCR < 0) and the insulator (TCR > 0). We

adopt this empirical ‘definition’ of the phases for the rest of this paper.

Examining Fig. 3 further reveals another transport feature which is typical to the QH-to-insulator transition. It is possible, at low  $T$ , to identify a clear and well-defined  $B$  value for which the TCR vanishes, within experimental error. The existence of this critical  $B$  value ( $B_c$ ) allows us to unambiguously determine (subject to the definition of the previous paragraph) the boundary between the QH state and the insulator. A complete phase diagram can be obtained by following the position of this ‘crossing’ point as other relevant parameters such as disorder or  $n$  is changed, as was done extensively by Wong *et al.*<sup>9</sup>, Song *et al.*<sup>38</sup> and others.

In a recent paper, Shahar *et al.*<sup>11</sup> reported on a study of the  $\rho_{xx}$  value at  $B_c$  ( $\rho_{xxc}$ ) for a large collection of samples. They noticed that, in accordance with theoretical expectations<sup>19</sup>,  $\rho_{xxc}$  seems to be close to the quantum unit or resistance,  $h/e^2$ , independent of sample parameters. Further, they showed that this apparent universality holds also for transitions from the  $1/3$  fractional QH state to the insulator, again in agreement with theoretical predictions<sup>18</sup>.

In the remainder of this section we expand on these previous findings by concentrating on the transport properties at the critical point. We will provide further evidence for the notion of universality near the QH-to-insulator transition, and remark on the QH-QH transitions. We will also closely examine the transport at the critical point and show that, at higher  $T$ ’s, systematic deviation of  $\rho_{xx}$  are clearly seen, although their trend and magnitude are sample dependent. Finally, we will discuss the disorder-driven QH-insulator transition which is realized experimentally by changing  $n$  by means of a metallic front-gate<sup>4</sup>. We will emphasize the similarities between the disorder and magnetic field driven transitions.

We would like to precede the discussion of our data with a note of caution. It would be an unreasonable expectation that *all* samples will behave uniformly in any subset of their transport characteristics. It is well-known, for instance, that samples exhibiting the FQHE do not undergo a transition from the  $\nu = 1$  IQHE to an insulator (they will, ultimately, undergo a transition to an insulator at higher  $B$  from a FQHE state). We therefore need to

define clearly which subset of our samples will be included in our test for universality at the QH to insulator transitions. To clarify this need we plot, in Fig. 4,  $B$  traces of  $\rho_{xx}$  taken at several  $T$ 's for a GaAs/AlGaAs sample grown on (311)A substrate to produce hole carriers. The “QH” state marked on the figure as  $1/3$  is clearly abnormal with a very high minimum resistivity at the lowest  $T$ . It is not surprising that the following “transition” (common crossing point of the different  $T$  traces) to an insulator is at a very high value,  $\rho_{xxc} = 220$  k $\Omega$ , which significantly deviates from universality. The above discussion leads to a natural, albeit arbitrary, criterion for the “suitability” of a given transition for a test of universality: For a transition to be considered, we require that it exhibit a fully developed QH state followed by a strong insulating behavior.<sup>39</sup> In both cases different tests can be considered to define the “strength” of the phase, and we chose for the QH a resistivity that decrease exponentially with decreasing  $T$  and, in addition, a value of  $\rho_{xx}$  at the QH minimum which is less than  $h/100e^2$  at our lowest  $T$ , such that it is undecernable from zero when plotted on a scale which includes the transition point. Similarly we defined a fully developed insulator if  $\rho_{xx}$  increases monotonously with  $B$  and  $T$  and reaches a value greater then  $100h/e^2$  at our lower  $T$ . Arbitrary as they are, these simple criteria safely eliminate from consideration samples like that of Fig. 4.

In a previous letter<sup>11</sup> we reported the observation of a universal value of  $\rho_{xxc}$ . In Fig. 5 we plot  $\rho_{xxc}$  vs.  $B_c$  for 20 of our samples. In fact, other absisca could have equally been used, such as  $\mu$  or  $n$ , as  $\rho_{xxc}$  is rather independent of sample parameters and appears to be scattered around  $h/e^2$  (solid line in Fig. 5). Two points should be emphasized. First, as we noted before, the  $\rho_{xxc}$  value is not significantly different between samples that undergo the transition from the  $\nu = 1$  integer QH state (empty symbols) and those for which the transition takes place from the  $\nu = 1/3$  fractional QH state (solid symbols). This is in agreement with the theoretical notion of super-universality<sup>18</sup>. We will not be discussing fractional QH transitions in the remainder of this paper.

Second, the data points are scattered over a relatively wide range of  $\approx 25\%$  around  $h/e^2$ . This scatter is evident not only for different samples but also for different cool-downs of the

same sample. This cool-down dependence of  $\rho_{xxc}$  is particularly puzzling if we recall that are samples are all of rather large size. This point has been emphasized in our previous publication, and is not yet understood theoretically.

So far, we reviewed our definition of the transition  $B_c$  and discussed the low- $T$  value of  $\rho_{xxc}$ . We now proceed to discuss the  $T$ -dependence of  $\rho_{xxc}$  at higher  $T$ 's. In Fig. 6 we plot  $\rho_{xxc}$  vs.  $T$  for several samples. Depending on the sample and the  $T$  range at hand, different forms of behavior are observed. Common to all samples is a certain range at the lowest  $T$  where  $\rho_{xxc}$  is  $T$  independent, as expected at the critical point of the transition. This value of  $\rho_{xxc}$  is the value plotted in Fig. 5. As  $T$  is increased, systematic deviations are observed in most samples. The  $T$  where these deviations appear is sample dependent, as is the trend which they take. In 7 we plot  $\rho_{xxc}$  vs.  $T$  on a log scale which shows that for this particular sample, where we have a relatively wide range of data, a logarithmic  $T$  dependence of  $\rho_{xxc}$  is a reasonable description of the data. This dependence is similar to that observed for 2D disordered metals at low  $T$  and  $B = 0$ . It is not clear whether the various mechanisms that lead to the logarithmic  $T$ -dependence at  $B = 0$  are applicable for the high- $B$  case.

In the limit of strong disorder, the QH ceases to exist and is replaced with an insulating behavior. It is a reasonable expectation, that if one could vary the effective disorder over a wide enough range, a transition from a QH state to an insulator will be observed. This expectation was verified in experiments<sup>4-6</sup>. In fact, the disorder-induced transition was shown to be remarkably similar to the  $B$ -field-induced one as far as its critical properties are concerned<sup>9</sup>. To vary the effective disorder the experimentalist usually employs a metallic gate deposited near the 2D electrons. By biasing the gate with respect to the electron system  $n$  can be varied continuously, resulting in an effective disorder change via the dependence of the impurities potential-strength on the screening effectiveness of the electrons which, in turn, depends on  $n$ . In Fig. 8 we plot  $\rho_{xxc}$  vs.  $T$  in the vicinity of a disorder-induced  $\nu = 1$  to insulator transition. The different sets of data correspond, in this figure, to different gate-voltage bias and therefore to different disorder. The qualitative similarity to the  $B$  induced transition is clear. In addition we note that  $\rho_{xxc}$  for this transition is  $\sim 24\text{k}\Omega$ , again

close to  $h/e^2$ . The  $T$  range of our study in this case is not sufficient to detect the high- $T$  deviations of  $\rho_{xx}$ .

Finally we remark on the behavior at the critical point of QH-QH plateau-to-plateau transitions. As we demonstrated in a recent paper<sup>14</sup>, a direct and clear relation exist between these transitions: It is possible to map the QH-to-insulator transition to a QH-QH transition by considering the former as a QH-insulator transition occurring at the top LL in the presence of an inert (full) bottom LL. In Ref.<sup>14</sup> we found that the transition point, when properly identified, is at a value which is close (within 20%) to the theoretically predicted value of  $1/5 h/e^2$  (See Fig 9). Many other samples exhibit QH-QH with  $\rho_{xx}$  much smaller than expected. We are uncertain why the QH-insulator transition yields a more consistent critical behavior than the QH-QH case.

### III. NUMERICAL STUDY OF THOULESS CONDUCTANCE

In this section we present results of numerical studies of the Thouless conductance at the critical point, using a non-interacting electron model on a square lattice, described by the following Hamiltonian:

$$H = \sum_{m,n} \{ -(c_{m+1,n}^\dagger c_{m,n} + c_{m,n+1}^\dagger e^{i2\pi\alpha m} c_{m,n} + \text{H.c.}) + \epsilon_{m,n} c_{m,n}^\dagger c_{m,n} \}, \quad (1)$$

where the integers  $m$  and  $n$  are the  $x$  and  $y$  coordinates of the lattice site in terms of lattice constant,  $c_{m,n}$  is the fermion operator on that site, H.c. stands for Hermitian conjugate,  $\alpha$  is the amount of magnetic flux per plaquette in units of the flux quantum  $hc/e$ , and  $\epsilon$  is the random onsite potential. We will present data mostly for uncorrelated random potential (i.e., no correlation between  $\epsilon$ 's on different lattice sites), with  $\epsilon$  ranging uniformly from  $-W$  to  $W$ . Random potential with some short range correlation will also be studied. The Landau gauge  $\mathbf{A} = (0, Bx, 0)$  is used in Eq. (1). In this work we study finite size systems of square geometry, with linear size  $L$ , for  $L$  ranging from 18 to 50. We impose periodic boundary condition (PB) along the  $\hat{x}$  direction:  $\Psi(k + L\hat{x}) = e^{i\phi_1} \Psi(k)$ , and periodic or



antiperiodic boundary condition (APB) along the  $\hat{y}$  direction:  $\Psi(k + L\hat{y}) = \pm\Psi(k)$ . We diagonalize the Hamiltonian (1) numerically to obtain the single-electron spectrum for both the periodic boundary condition ( $E_p^n$ ), and antiperiodic boundary condition ( $E_{ap}^n$ ) along  $\hat{y}$  direction, while keeping the boundary condition along  $\hat{x}$  to be periodic. Here  $n$  is the index for a specific eigenstate.

The Thouless conductance<sup>48</sup> at Fermi energy  $E$  is defined as

$$g_T(E) = \frac{\langle\delta E\rangle}{\Delta E}, \quad (2)$$

where  $\Delta E = 1/[L^2 D(E)]$  is the average level spacing at  $E$ , determined by the disorder averaged density of states (DOS) per site  $D(E)$ , and  $\langle\delta E\rangle$  is the average of the absolute value of the difference between  $E_p^n$  and  $E_{ap}^n$ , also at energy  $E$ .<sup>49</sup>

In Fig. 10 we show the Thouless conductance ( $g_T$ ) for systems with  $\alpha = 1/3$ ,  $W = 2.5$  (uncorrelated potential), and  $L$  ranging from 18 to 48. We find except for 4 special energies,  $g_T$  decreases as  $L$  increases; while for  $E = \pm E_c^1 \approx \pm 2.0$  and  $E = \pm E_c^2 \approx \pm 1.1$ ,  $g_T$  peaks, and appears to be essentially *independent* of  $L$ .<sup>50</sup> The physics of such behavior may be understood in the following way.<sup>30–34</sup> In the absence of random potential we have three Landau subbands, and the Hall conductance (in unit of  $e^2/h$ ) for each subband is 1 for the two side bands and  $-2$  for the central band. As random potential is turned on, most states get localized, but there will be one critical energy in each side band ( $\pm E_c^1$ ) and two critical energies ( $\pm E_c^2$ ) in the central band, at which states are delocalized. The Hall conductance carried by the extend states is 1 for  $\pm E_c^1$ , and  $-1$  for  $\pm E_c^2$ . For energies away from these critical energies states are localized, therefore  $g_T$  decreases as system size  $L$  increases, and goes to zero in the thermodynamic limit; at these critical energies states are delocalized, and  $g_T$  approaches a finite number in the thermodynamic limit; for large enough system size  $L$ ,  $g_T$  is essentially independent  $L$ . It is clear from the plot that  $g_T$  has essentially reached its asymptotic value for  $L \geq 18$ ; the size dependence of  $g_T$  at smaller sizes will be discussed later.  $E_c^1$  and  $E_c^2$  move together as  $W$  increases, and at  $W = W_c \approx 2.9$  they merge together and kill each other, and all states become localized.<sup>32</sup>

In the following we will focus on the value of  $g_T$  at the critical energies. In Fig. 11a we show the size-independent peak value of  $g_T$  at  $E = -E_c^1$ , for different randomness strength  $W$ 's, and  $L = 30$  (which we believe to be in the asymptotic regime already). The value of  $g_T$  is the same at  $E = E_c^1$ , due to particle-hole symmetry of the model. We find  $g_T \approx 0.21 \pm 0.02$ , *independent* of the value of  $W$ . In Fig. 11b we present the peak value of  $g_T$  in the lowest Landau subband for  $\alpha = 1/5$  and  $\alpha = 1/7$ , at different  $W$ 's, and system sizes  $L = 25$  and  $L = 21$  respectively. We have checked that for these sizes the peak value of  $g_T$  of the lowest Landau subband is already at its asymptotic value. Again we get the same value, within error bars, even though we have different field strength and different number of Landau subbands.

So far we have only studied uncorrelated random potentials on the lattice, which maps onto Gaussian white noise potential in the continuum limit. In the following we study random potentials with short-range correlations. We use the following way to generate short-range correlation: numerically we generate an uncorrelated random number  $w_i$ , uniformly distributed from  $-W$  to  $W$ , for each lattice site  $i$ . Instead of using  $w_i$  as the random potential  $\epsilon_i$  as before, we take

$$\epsilon_i = w_i + a \sum_{\delta} w_{i+\delta}, \quad (3)$$

where the summation is over the four neighboring sites of  $i$ . This way the potential of one site is correlated with its nearest and next nearest neighbors, and the amount of correlation is determined by  $a$ . In Fig. 12 we show the size-independent peak value of  $g_T$  (again based on data with  $L = 30$ ) at  $E_c^1$ , for  $\alpha = 1/3$ ,  $W = 1.5$ , at different  $a$ 's. We find within error bars it is independent of  $a$ , and takes the same value as the uncorrelated potential ( $a = 0$ ).

Our data clearly indicates that  $g_T \approx 0.21 \pm 0.02$  is a universal number at the critical energy of the lowest Landau subband of the square lattice, independent of the strength of the randomness and magnetic field, as well as the type of random potential (correlated or uncorrelated). Within error bars, the same universal number is also found in the lowest Landau level of the *continuum system* in Ref. 35, where the same definition of the Thouless

conductance was used. We point out however that in our calculation, no projection to individual subbands is made, and mixing between different Landau subbands (or levels) (which is often important in real systems) is taken into account. We thus conclude that just like the conductivity tensor, the Thouless conductance is a universal number at integer quantum Hall transition in noninteracting electron models (either on a lattice or in the continuum).

In principle, the truly universal value of  $g_T$  at the critical energies is reached in the thermodynamic limit  $L \rightarrow \infty$  only; there is always finite size correction of  $g_T$  at finite  $L$ , and the correction should decrease as  $L$  increases. As discussed in section I, in a noninteracting system a finite system size is equivalent to finite temperature in an infinite system. Since real experiments are always done at finite temperatures, such finite size effects are observable. Motivated by this we have also studied the size dependence of  $g_T$  at the critical energies. In Fig. 13 we plot the dependence of  $g_T$  at  $E = -E_c^1$  for  $\alpha = 1/3$  and  $W = 2.5$ . We find, quite remarkably, that for  $L$  as small as 9,  $g_T$  has essentially saturated at the asymptotic value, indicating that the finite size corrections of  $g_T$  disappear extremely fast as  $L$  increases. The deviation of  $g_T$  at  $L = 6$  from the universal value is clearly due to finite size corrections; associated with that, we have also found strong dependence of the peak value of  $g_T$  at  $L = 6$  on the randomness strength  $W$ , as shown in Fig. 14. We find the bigger  $W$  is, the closer to the universal value  $g_T$  becomes. This is reasonable because the stronger randomness is more effective in localizing states away from critical energies, and therefore suppress finite size effects. No such dependence on  $W$ , however, is found for larger  $L$  where  $g_T$  has saturated at the universal value.

In the RG language, the finite size corrections to universal properties at the critical point is due to the existence of irrelevant operators, whose strength scales to zero in the thermodynamic limit under RG at the critical point, while they remain finite in finite size systems. It has been known<sup>51</sup> for some time now, based on numerical studies, that the length scale required for such irrelevant operators to scale away is quite small in the lowest Landau level, while in higher Landau levels it becomes very large. The origin of this difference is

not yet fully understood. Our results in the lowest Landau subband is clearly consistent with this finding. Also consistent with this, we do see some weak size dependence of the peak value of  $g_T$  in higher subbands (see Fig. 10), suggesting the existence of finite size correction in the size range of our numerical study. We have also found strong dependence of the peak value of  $g_T$  in higher subbands on  $W$  for a given size as shown in Fig. 15. The dependence is very similar to that of the peak value of  $g_T$  in the lowest subband with  $L = 6$ , where we know finite size corrections are present. Based on these we conclude that finite size corrections are quite important in higher Landau subbands within the size range of the present study, and conjecture that in the thermodynamic limit, the peak value of  $g_T$  will saturate at the same universal value as in the lowest subband, provided that the critical energy carries Hall conductance  $\pm 1$ . We will discuss the possible experimental consequences of these finite size effects in section IV.

#### IV. SUMMARY AND DISCUSSIONS

In this paper we have presented results of detailed experimental studies on the universality of the resistivity tensor at the quantum critical points separating an integer quantum Hall phase and the high magnetic field insulator, as well as critical points separating different integer quantum Hall phases. Our results strongly suggest that the resistivity tensor is universal at the critical points, and that quantum Hall-insulator and quantum Hall-quantum Hall transitions are in the same universality class. This is in agreement with previous experimental studies, as well as general theoretical expectations.

We have also studied such transitions using a non-interacting electron model on a lattice, and found that the Thouless conductance at the critical points is universal. This is in agreement with our experimental findings, as well as previous theoretical studies using different models and approaches. It has been known for a long time that the Thouless conductance is closely related to the longitudinal conductivity of the system; they are believed to be of the same order of magnitude, no matter the system is in the insulating phase, metallic phase, or

at the critical point, and are roughly proportional to each other. People have not succeeded, however, in establishing an exact relation between these two quantities in general. If both of them are universal at the critical point, their ratio must also be universal at the critical point. Since numerically the Thouless conductance is much easier to calculate than the longitudinal conductivity, such a simple relation should be very useful in future researches. It will also be very interesting to see if the same ratio relates these two quantities away from the critical point.

We have also, probably for the first time in the literature, presented a detailed analysis on how the universal values of the resistivity tensor are approached in the asymptotic low temperature regime, and the deviation from the universal values at higher temperatures. We find that the longitudinal resistivity  $\rho_{xx}$  at the critical point has some sizable, and apparently non-systematic deviation from the universal value at relatively high temperatures; while the Hall resistivity  $\rho_{xy}$  has essentially no such deviation in the same temperature range. Using the relation between the resistivity and conductivity tensors:

$$\rho_{xx} = \frac{\sigma_{xx}}{\sigma_{xx}^2 + \sigma_{xy}^2}, \quad (4)$$

$$\rho_{xy} = \frac{\sigma_{xy}}{\sigma_{xx}^2 + \sigma_{xy}^2}, \quad (5)$$

we find the deviation of  $\rho_{xx}$  and  $\rho_{xy}$  from the universal values are related to the deviation of  $\sigma_{xx}$  and  $\sigma_{xy}$  to the lowest order<sup>52</sup> in the following way:

$$\delta\rho_{xx} \approx \frac{1}{\sigma_{xx}^2 + \sigma_{xy}^2} \left[ \delta\sigma_{xx} \left( 1 - \frac{2\sigma_{xx}^2}{\sigma_{xx}^2 + \sigma_{xy}^2} \right) - \delta\sigma_{xy} \frac{2\sigma_{xy}^2}{\sigma_{xx}^2 + \sigma_{xy}^2} \right], \quad (6)$$

$$\delta\rho_{xy} \approx \frac{1}{\sigma_{xx}^2 + \sigma_{xy}^2} \left[ \delta\sigma_{xy} \left( 1 - \frac{2\sigma_{xy}^2}{\sigma_{xx}^2 + \sigma_{xy}^2} \right) - \delta\sigma_{xx} \frac{2\sigma_{xx}^2}{\sigma_{xx}^2 + \sigma_{xy}^2} \right]. \quad (7)$$

Since at the integer quantum Hall-insulator transition  $\sigma_{xx} = \sigma_{xy} = 0.5e^2/h$ , we find

$$\delta\rho_{xx} \approx -\delta\sigma_{xy}(2h^2/e^4), \quad (8)$$

$$\delta\rho_{xy} \approx -\delta\sigma_{xx}(2h^2/e^4). \quad (9)$$

Thus the deviation of *longitudinal* resistivity  $\delta\rho_{xx}$  at finite  $T$  is proportional to the deviation of *Hall* resistivity  $\delta\sigma_{xy}$ , while the absence of deviation in *Hall* resistivity implies the deviation

of *longitudinal* conductivity  $\delta\sigma_{xx} \approx 0$ ! In our numerical study on Thouless conductance, we have already seen that the Thouless conductance, which is believed to be proportional to  $\sigma_{xx}$ , approaches the universal value at extremely small system sizes at the critical point; this naturally explains the fact  $\delta\sigma_{xx} \approx 0$  and hence the absence of deviation in  $\rho_{xx}$  at finite  $T$  at the critical point. In a noninteracting electron model,  $\delta\sigma_{xy}$  at the critical point due to finite size effects can only come from particle-hole (PH) asymmetry in the corresponding Landau level (band). Both PH asymmetry in the underlying potential, and mixing of different Landau levels (bands), can give rise to such asymmetry. A detailed numerical study on the effects of PH asymmetry on  $\delta\sigma_{xy}$  at the critical point in finite size systems will be presented elsewhere.

Quantum phase transitions is a fascinating subject, and we expect study of quantum Hall transitions continues to be a fruitful field of research.

## ACKNOWLEDGMENTS

This work was supported by NSF grant DMR-9400362.

## REFERENCES

- <sup>1</sup> For a recent review that is particularly relevant to the present work, see S. L. Sondhi, S. M. Girvin, J. P. Carini and D. Shahar, Rev. Mod. Phys. **69**, 315 (1997).
- <sup>2</sup> H. P. Wei, D. C. Tsui, M. A. Paalanen and A. M. M. Pruisken, Phys. Rev. Lett. **61**, 1294 (1988).
- <sup>3</sup> S. Koch *et al.*, Phys. Rev. Lett. **67**, 883 (1991).
- <sup>4</sup> H. W. Jiang *et al.*, Phys. Rev. Lett. **71**, 1439 (1993).
- <sup>5</sup> T. Wang *et al.*, Phys. Rev. Lett. **72**, 709 (1994).
- <sup>6</sup> R. J. F. Hughes *et al.*, J. Phys. Condens. Matter **6**, 4763 (1994).
- <sup>7</sup> B. W. Alphenaar and D. A. Williams, Phys. Rev. B **50**, 5795 (1994).
- <sup>8</sup> H. P. Wei *et al.*, Phys. Rev. B **50**, 14609 (1994).
- <sup>9</sup> L. W. Wong, H. W. Jiang, N. Trivedi and E. Palm, Phys. Rev. B **51**, 18033 (1995).
- <sup>10</sup> W. Pan, D. Shahar, D. C. Tsui, H. P. Wei and M. Razeghi, Phys. Rev. B **55**, 15431 (1997).
- <sup>11</sup> D. Shahar, D. C. Tsui, M. Shayegan, R. N. Bhatt and J. E. Cunningham, Phys. Rev. Lett. **74**, 4511 (1995).
- <sup>12</sup> T. Okamoto, Y. Shinohara and S. Kawaji, Phys. Rev. B **52**, 11109 (1995).
- <sup>13</sup> D. Shahar, D. C. Tsui, M. Shayegan, J. E. Cunningham, E. Shimshoni and S. L. Sondhi, Science **274**, 589 (1996).
- <sup>14</sup> D. Shahar, D. C. Tsui, M. Shayegan, E. Shimshoni and S. L. Sondhi, Phys. Rev. Lett. **79**, 479 (1997).
- <sup>15</sup> J.T. Chalker and P.D. Coddington, J. Phys. C **21**, 2665 (1988).
- <sup>16</sup> B. Huckestein and B. Kramer, Phys. Rev. Lett. **64**, 1437 (1990).

- <sup>17</sup> Y. Huo and R.N. Bhatt, Phys. Rev. Lett. **68**, 1375 (1992).
- <sup>18</sup> S. Kivelson, D.H. Lee and S.-C. Zhang, Phys. Rev. B **46**, 2223 (1992).
- <sup>19</sup> Y. Huo, R. E. Hetzel and R. N. Bhatt, Phys. Rev. Lett. **70**, 481 (1993).
- <sup>20</sup> D.-H. Lee, Z. Wang and S. Kivelson, Phys. Rev. Lett. **70**, 4130 (1993).
- <sup>21</sup> Z. Wang, D.-H. Lee and X.-G. Wen, Phys. Rev. Lett. **72**, 2454 (1994).
- <sup>22</sup> D. Liu and S. Das Sarma, Phys. Rev. B **49**, 2677 (1994).
- <sup>23</sup> A. W. W. Ludwig, M. P. A. Fisher, R. Shankar and G. Grinstein, Phys. Rev. B **50**, 7526 (1994).
- <sup>24</sup> S.-R. E. Yang, A. H. MacDonald and B. Huckestein, Phys. Rev. Lett. **74**, 3229 (1995).
- <sup>25</sup> D.-H. Lee and Z. Wang, Phys. Rev. Lett. **76**, 4014 (1996).
- <sup>26</sup> D.-H. Lee and Z. Wang, Phil. Mag. Lett. **73**, 145 (1996).
- <sup>27</sup> Z. Wang, B. Jovanovic and D.-H. Lee, Phys. Rev. Lett. **77**, 4426 (1996).
- <sup>28</sup> S. Cho and M. P. A. Fisher, Phys. Rev. B **55**, 1637 (1997).
- <sup>29</sup> T. Ando, Phys. Rev. B **40**, 5325 (1989).
- <sup>30</sup> Y. Tan, J. Phys. Condens. Matter **6**, 7941 (1994).
- <sup>31</sup> D. Z. Liu, X. C. Xie and Q. Niu, Phys. Rev. Lett. **76**, 975 (1996).
- <sup>32</sup> Kun Yang and R.N. Bhatt, Phys. Rev. Lett. **76**, 1316 (1996).
- <sup>33</sup> X. C. Xie *et al.*, Phys. Rev. B **54**, 4966 (1996).
- <sup>34</sup> D. N. Sheng and Z. Y. Weng, Phys. Rev. Lett. **78**, 318 (1997).
- <sup>35</sup> E. S. Sorensen and A. H. MacDonald, Phys. Rev. B **54**, 10675 (1996).
- <sup>36</sup> S. Sachdev, preprint cond-mat/9709243 (1997).



- <sup>37</sup> D. N. Sheng and Z. Y. Weng, Phys. Rev. Lett. **80**, 580 (1998).
- <sup>38</sup> S. -H. Song, D. Shahar, D. C. Tsui, Y. H. Xie and D. Monroe, Phys. Rev. Lett. **78**, 2200 (1997).
- <sup>39</sup> As was recently noted by Shahar *et al.*<sup>40</sup>, it is not entirely clear whether in real samples  $\rho_{xx}$  indeed diverge in the  $T = 0$  limit, in the insulating phase near the transition point, nor is it clear that it vanishes in the QH phase. These observations are beyond the scope of the present discussion.
- <sup>40</sup> D. Shahar *et al.*, preprint (cond-mat/9706045).
- <sup>41</sup> M. P. A. Fisher, G. Grinstein and S. M. Girvin, Phys. Rev. Lett. **64**, 587 (1990).
- <sup>42</sup> P. A. Lee and T. V. Ramakrishnan, Rev. Mod. Phys. **57**, 287 (1985).
- <sup>43</sup> Y. Liu *et al.*, Phys. Rev. B **47**, (1993) and reference therein; A.F. Hebard and M.A. Paalanen, Phys. Rev. Lett. **65**, 927 (1990).
- <sup>44</sup> J.K. Jain, Phys. Rev. Lett. **63**, 199 (1989).
- <sup>45</sup> D. Simonian, S. V. Kravchenko and M. P. Sarachik, Phys. Rev. B **55**, R13421 (1997).
- <sup>46</sup> E. Abrahams *et al.*, Phys. Rev. Lett. **42**, 673 (1979).
- <sup>47</sup> D. Shahar, Ph.D. thesis, Princeton University (1996).
- <sup>48</sup> J. T. Edwards and D. J. Thouless, J. Phys. C **5**, 807 (1972); D. J. Thouless, Phys. Rep. **13**, 93 (1974).
- <sup>49</sup> There are different ways to define the Thouless conductance. For example, Ref. 24 uses the geometric mean instead of the ordinary average of the energy difference to determine  $\langle \delta E \rangle$ . What we mean by the universality of Thouless conductance is for a fixed definition, like the one used in this paper, the Thouless conductance at the critical point is independent of the details of the model.

<sup>50</sup> The independence of  $g_T$  on  $L$  is quite clear for  $E = \pm E_c^1$ , while at  $\pm E_c^2$  there appear to be some very weak  $L$  dependence. Based on previous studies (see below), we know that there should be two critical energies at  $\pm E_c^2$ . The weak size dependence of  $g_T$  on  $L$  will be discussed later.

<sup>51</sup> B. Huckestein, Phys. Rev. Lett. **72**, 1080 (1994).

<sup>52</sup> Since the observed deviation at finite  $T$  is typically of order one percent of the asymptotic value, expansion to the lowest order should be sufficient.

## FIGURES

FIG. 1. Mobility vs. density for some of the samples in this study. The vertical dashed line indicated by Max  $B$  represents the maximum density for which the QH-insulator transition can be observed in our 15.5 T magnet. The horizontal dashed line approximately separates samples that do not exhibit the fractional QH from those that do.  $p$ -type samples are circled, and the sample labeled 1/5 exhibit the reentrant insulating transition which we do not discuss in this paper.

FIG. 2.  $B$  traces of  $\rho_{xx}$  at  $T = 25, 42, 62, 84, 106, 125, 145, 194, 238, 284, 323$  mK, for a GaAs/AlGaAs sample mm051c.

FIG. 3. Same as Fig. 2 for a narrow  $B$  range focusing on the transition. We also included a  $\rho_{xy}$  trace (dashed curve).

FIG. 4.  $B$  traces of  $\rho_{xx}$  at  $T = 26, 46, 55, 99$  and  $177$  mK for a  $p$ -type GaAs/AlGaAs sample grown on (311)A substrate. Note the apparent crossing point at  $220$  k $\Omega$ .

FIG. 5.  $\rho_{xx}$  vs.  $B_c$  for some of our samples. Empty (filled) symbols are for transitions from the  $\nu = 1$  IQHE ( $\nu = 1/3$  FQHE) state. The error bars are typically smaller than the symbol size, except for the samples where they are indicated, which had ill-defined geometries.

FIG. 6.  $\rho_{xx}$  at  $B_c$ ,  $\rho_{xx}$ , vs.  $T$  for three of our samples. The dashed arrow indicates the theoretically predicted value for the transition,  $h/e^2$ . Sample m124u2d exhibit the fractional QH effect, and the data depicted is from the  $\nu = 1/3$ -insulator transition.

FIG. 7.  $\rho_{xxc}$  vs.  $T$  for sample c60ab, with a log- $T$  scale.

FIG. 8. Disorder-induced QH-insulator transition. Densities are, from top to bottom,  $0.7, 1.05, 1.3, 1.5, 1.7, 2.1, 2.9 \times 10^{10} \text{ cm}^{-2}$ .

FIG. 9.  $\rho_{xx}$  vs.  $T$  near a QH-QH transition. For this transition the predicted critical  $\rho_{xx}$  is  $1/5 h/e^2$ .

FIG. 10. Thouless conductance  $g_T$  as a function of energy for  $\alpha = 1/3$ ,  $W = 2.5$ , at different system sizes.

FIG. 11. Peak value of the Thouless conductance  $g_T$  in the lowest Landau subband, for different magnetic field ( $\alpha$ ) and randomness ( $W$ ) strength, with uncorrelated random potential.

FIG. 12. Peak value of the Thouless conductance  $g_T$  in the lowest Landau subband for short-range correlated potential.  $a$  is the strength of short-range correlation.

FIG. 13.  $L$  dependence of  $g_T$  at the critical energy of the lowest Landau subband for  $\alpha = 1/3$ .

FIG. 14. The peak value of  $g_T$  (at  $E = -E_c^1$ ) in the lowest Landau subband for  $\alpha = 1/3$  and  $L = 6$  versus randomness strength  $W$ .

FIG. 15. The peak value of  $g_T$  (at  $E = -E_c^2$ ) in the central Landau subband for  $\alpha = 1/3$  and  $L = 30$  versus randomness strength  $W$  ( $E_c^2$  depends on  $W$ ).

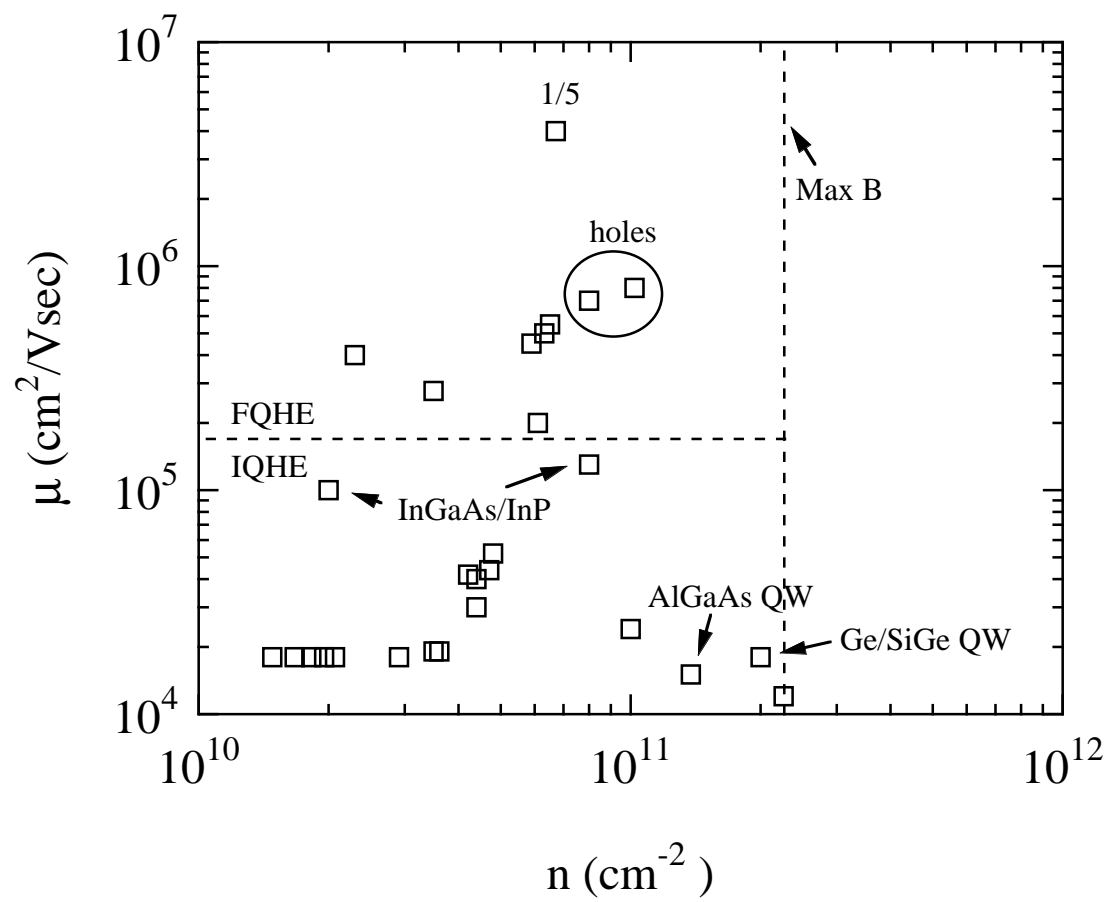


Fig. 1.

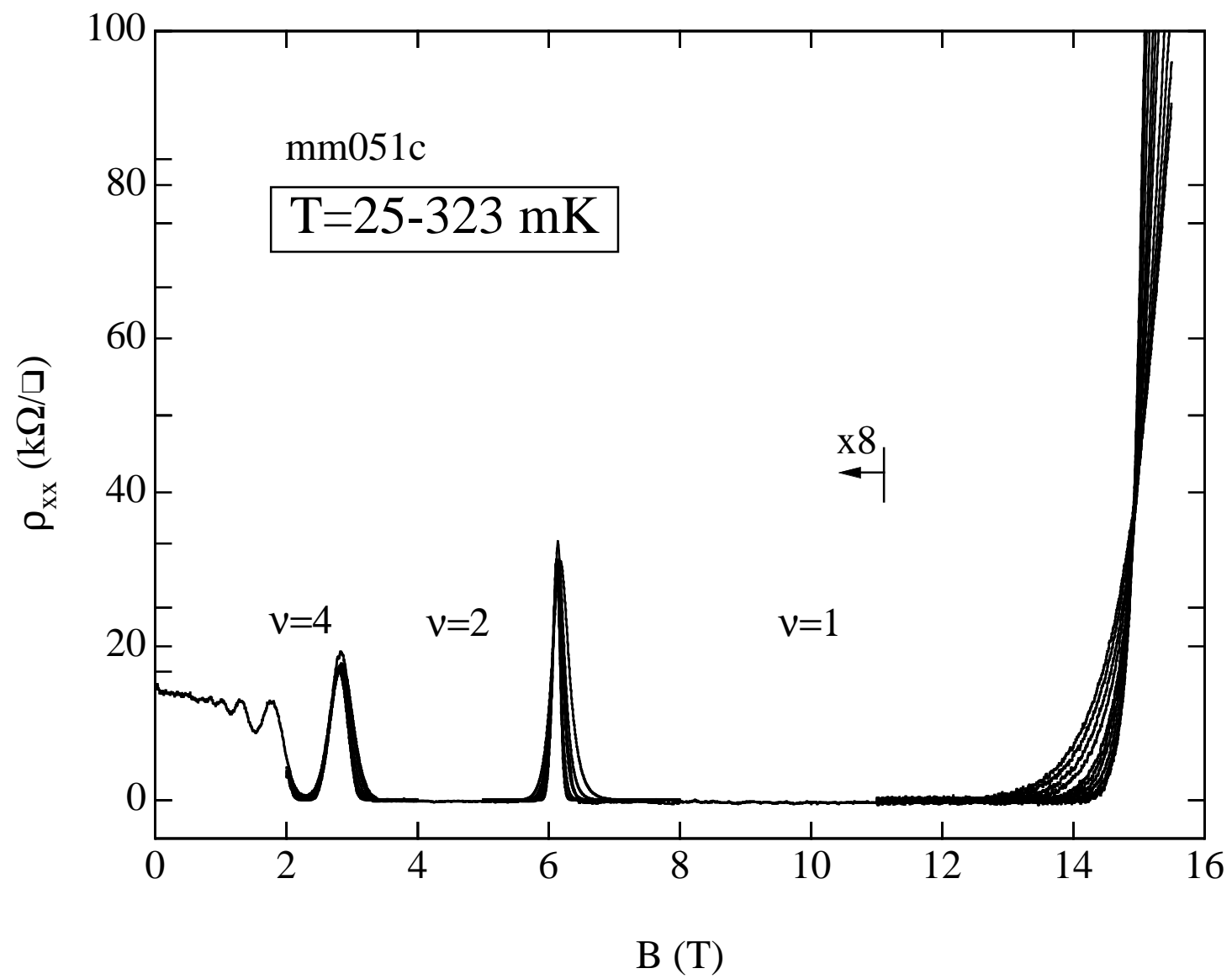


Fig. 2

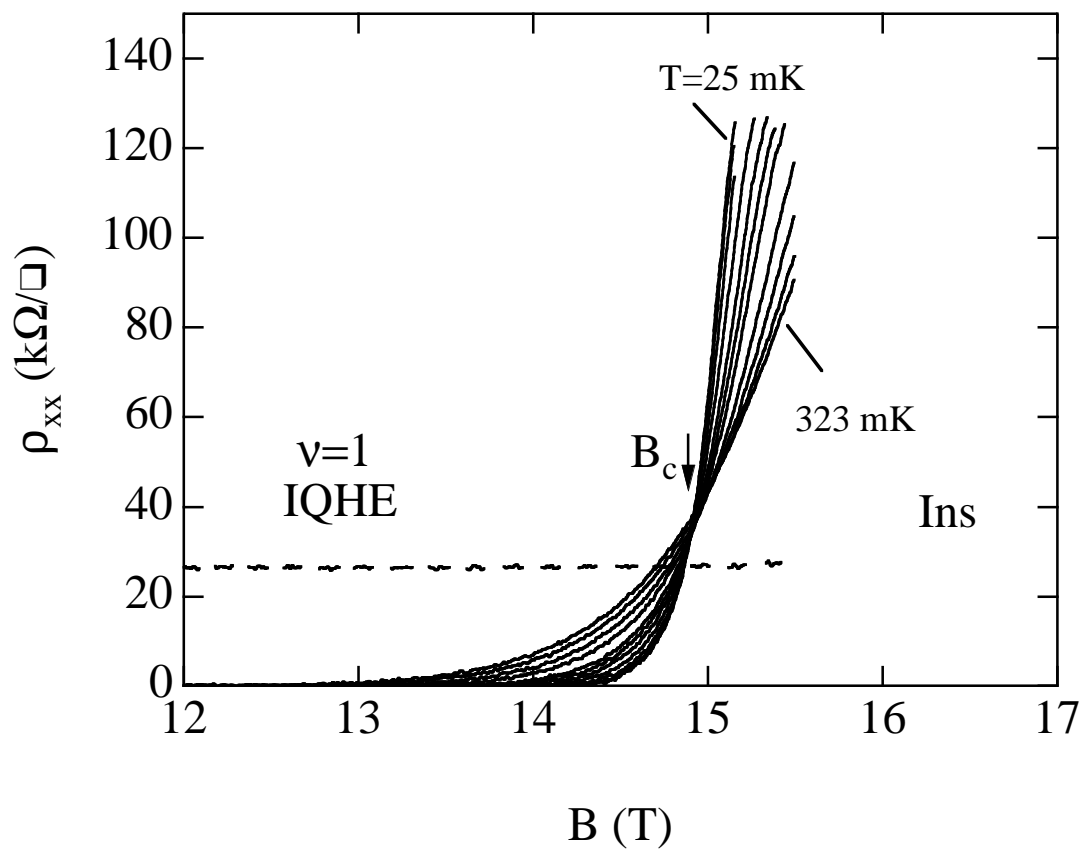


Fig 3.

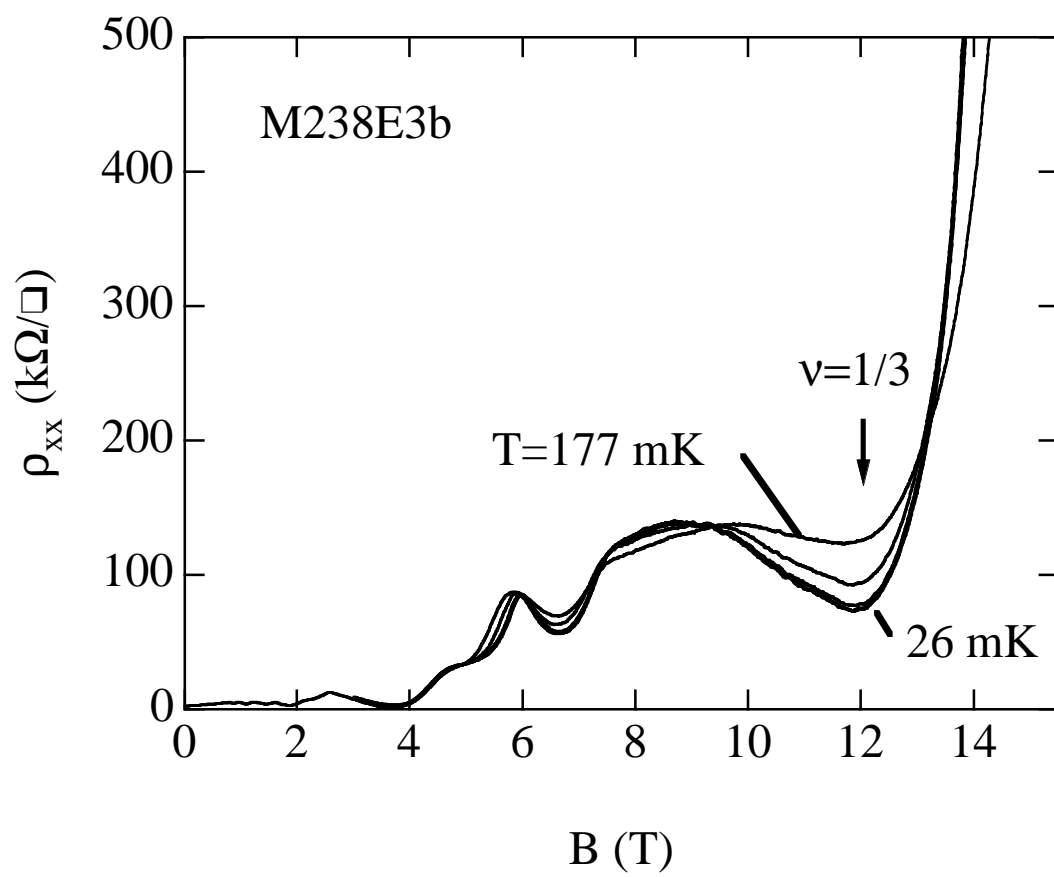


Fig 4.



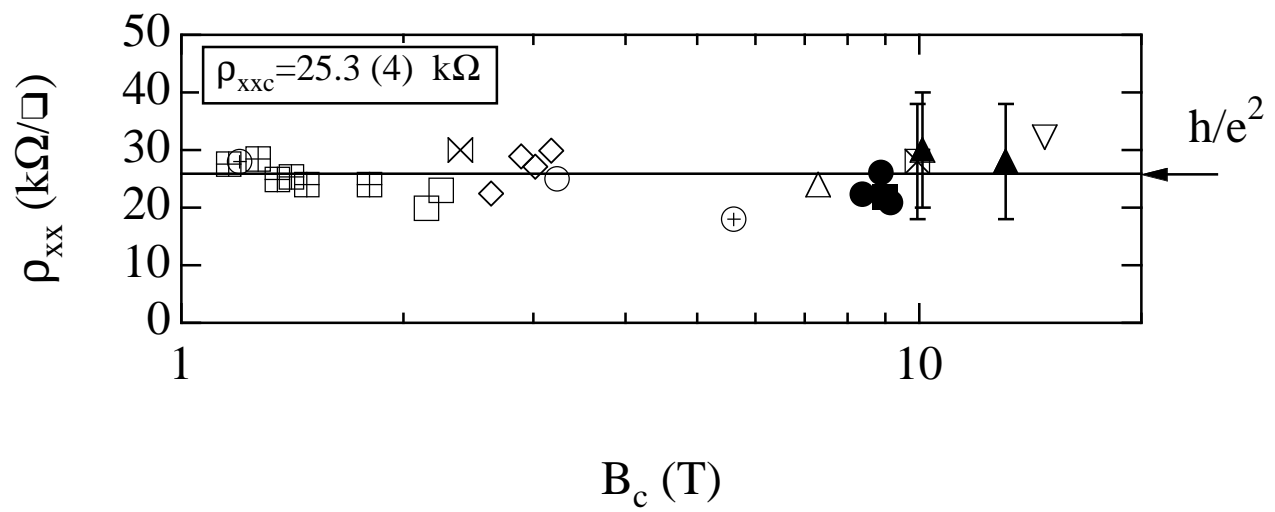


Fig. 5.

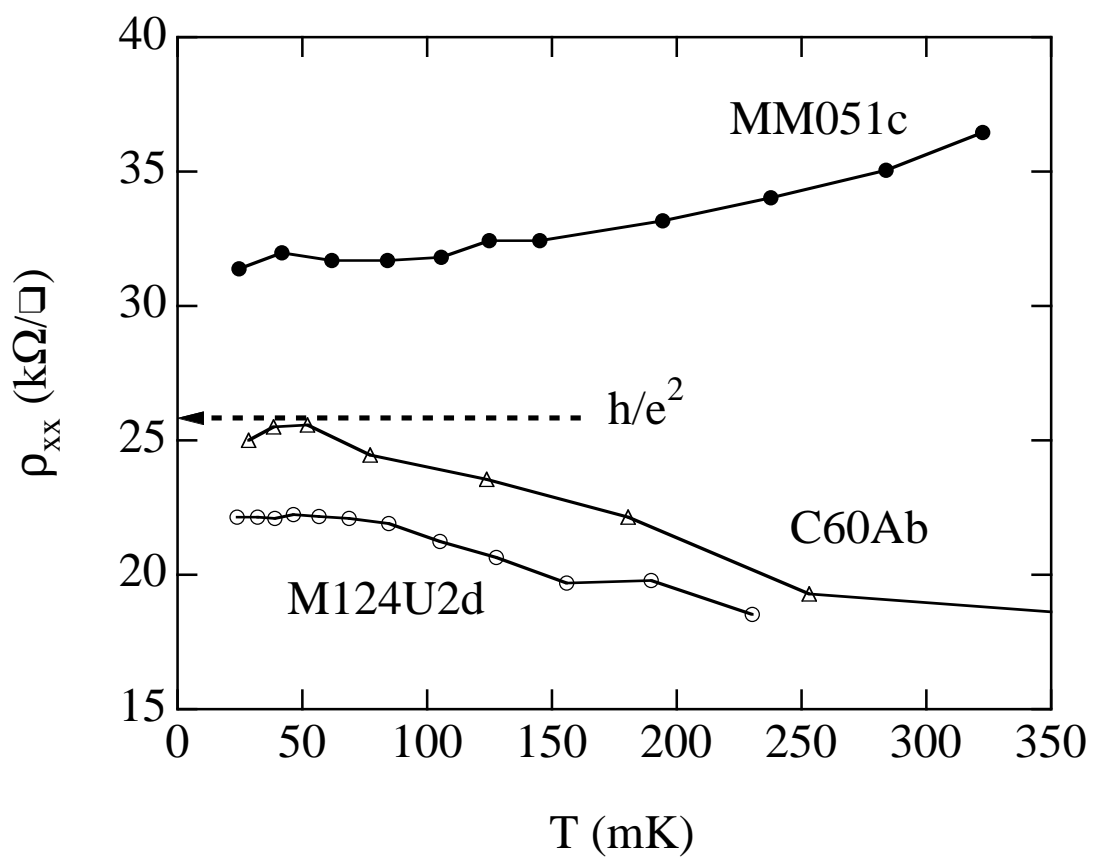


Fig 6

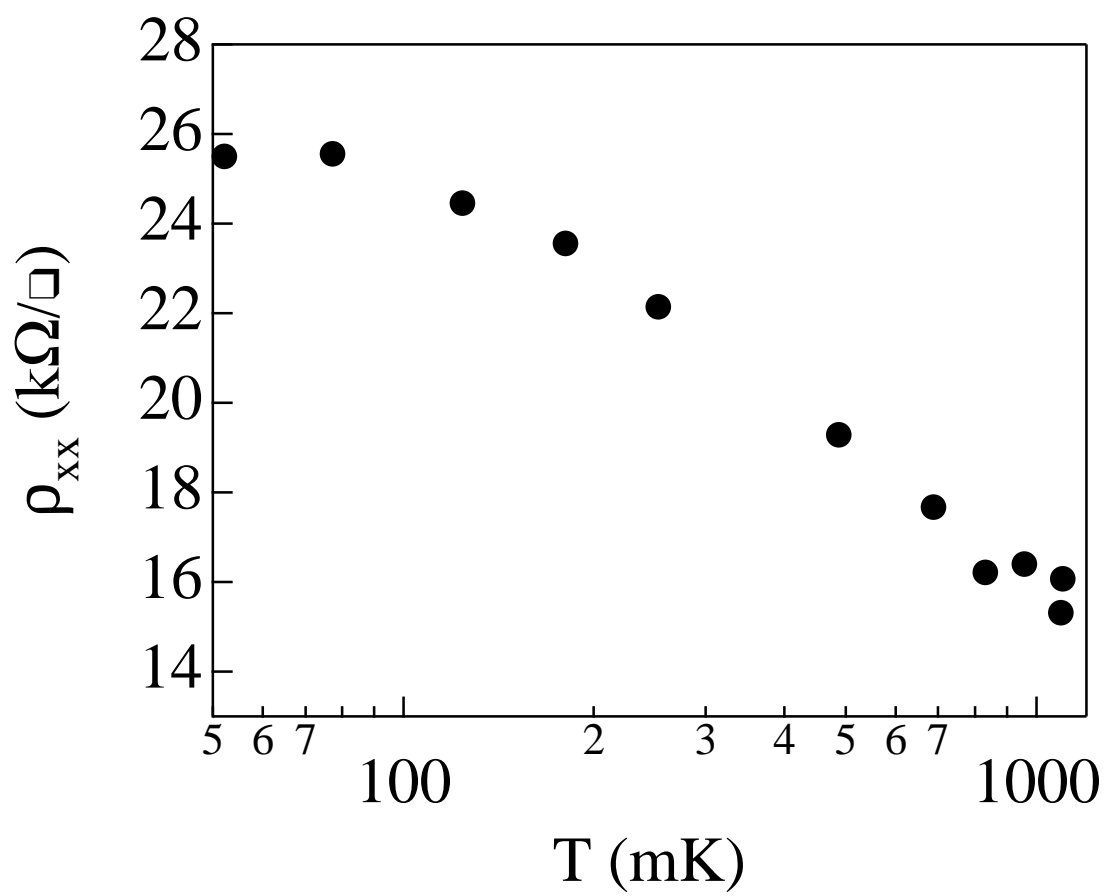


Fig. 7.

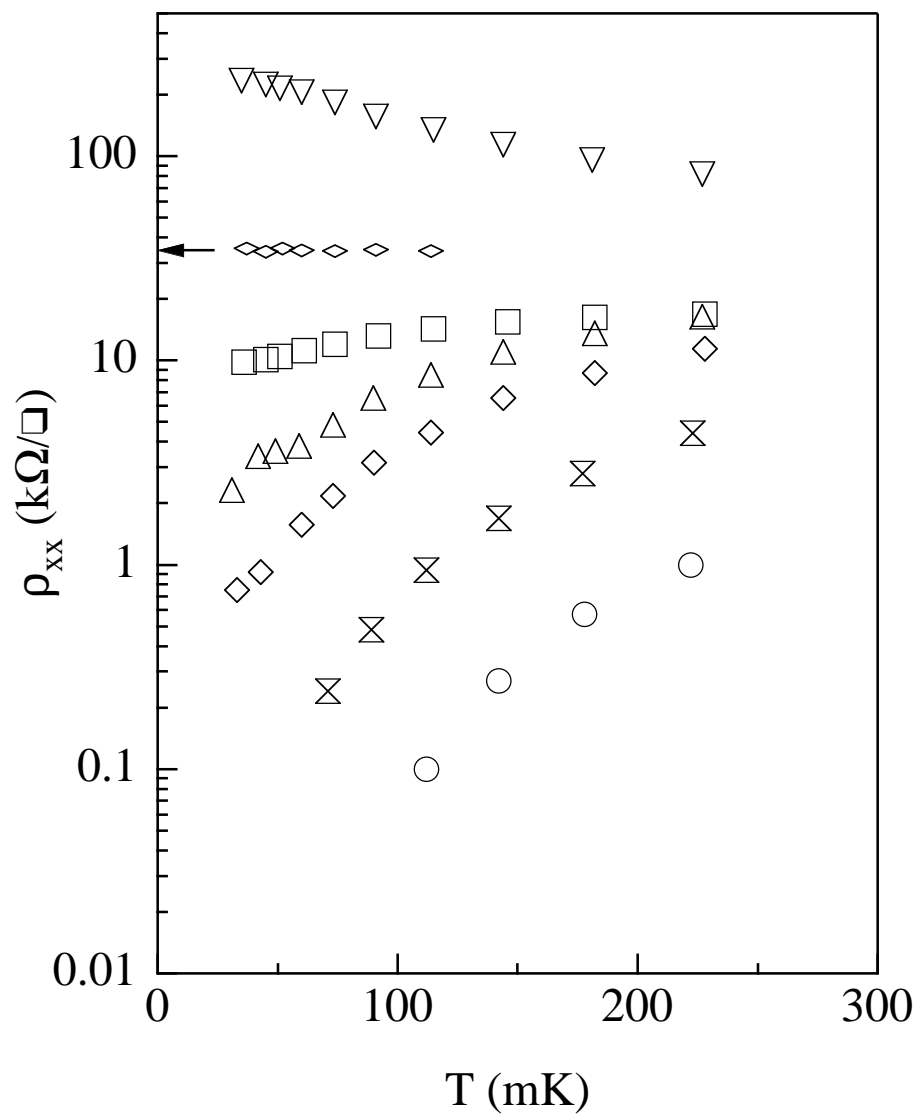


Fig. 8.

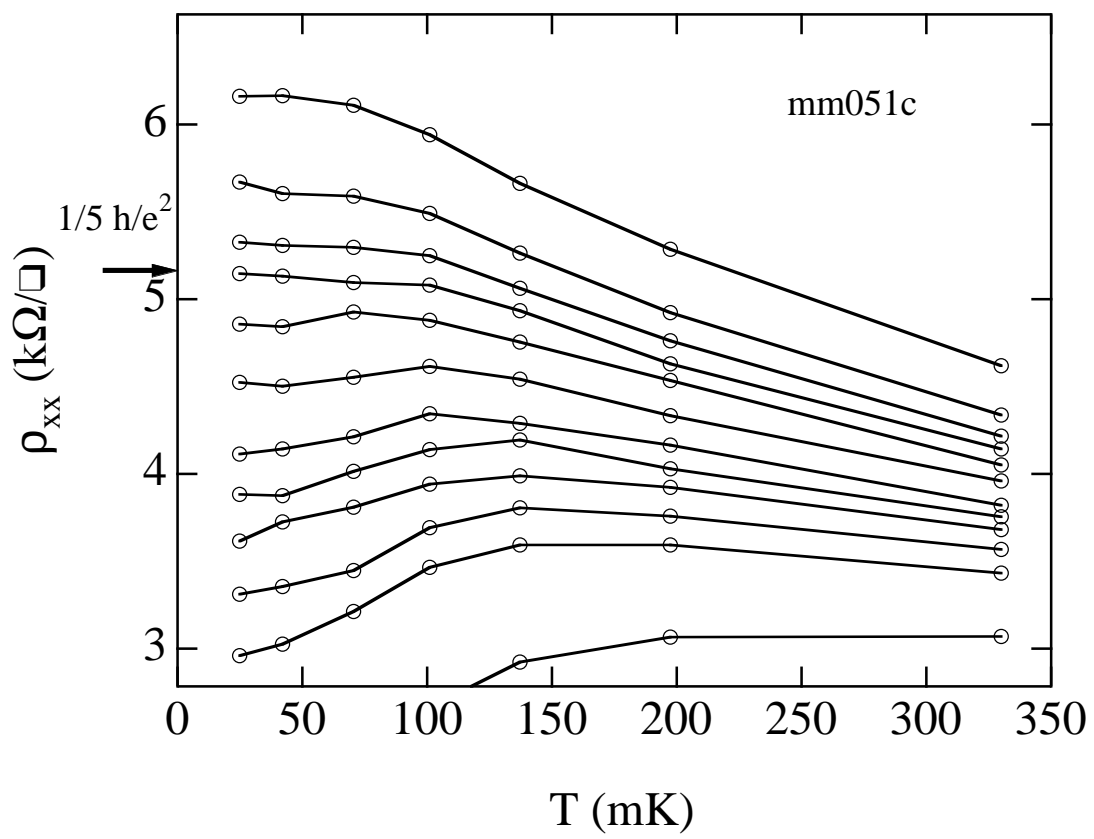


Fig. 9.

Fig. 10

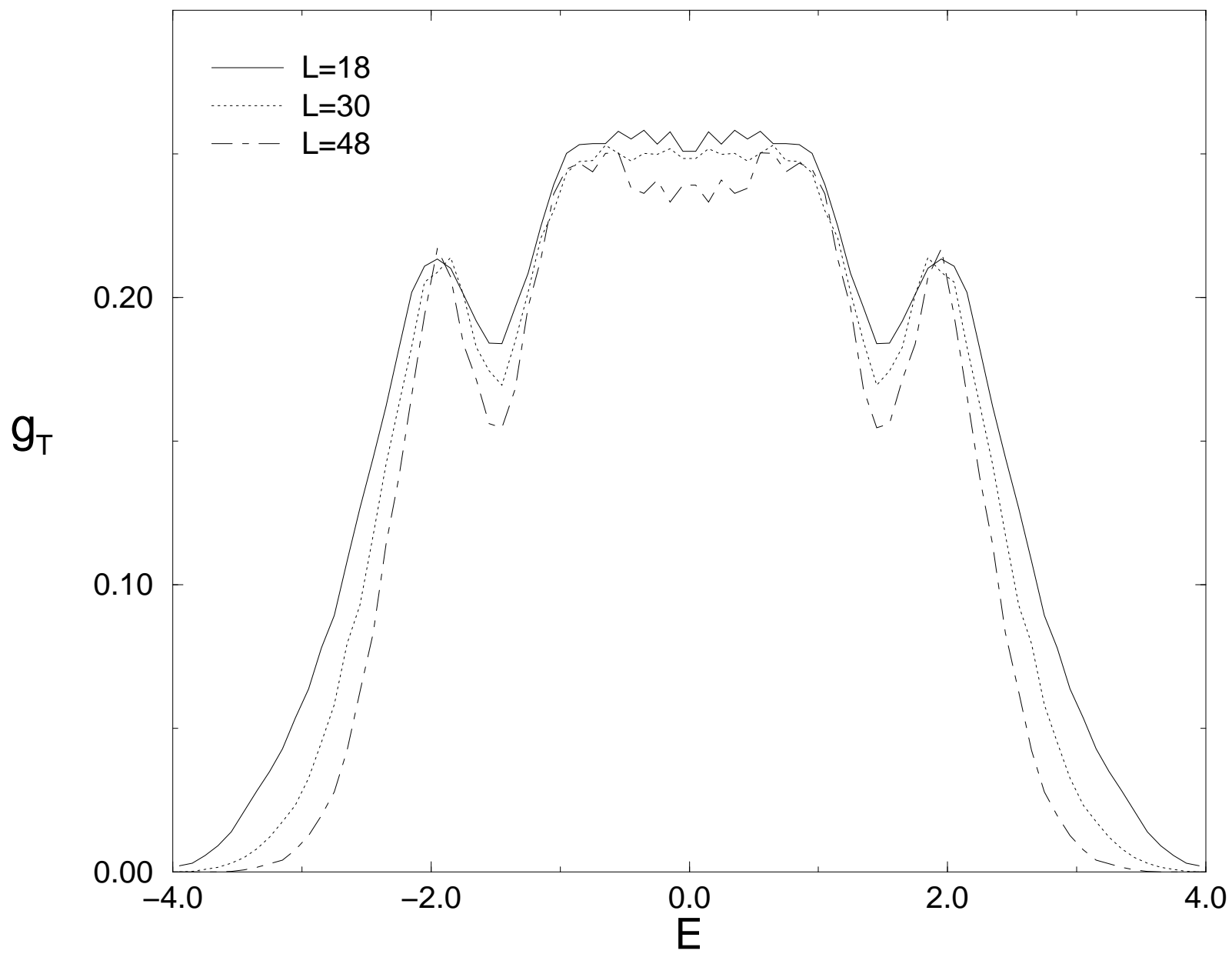


Fig. 11a

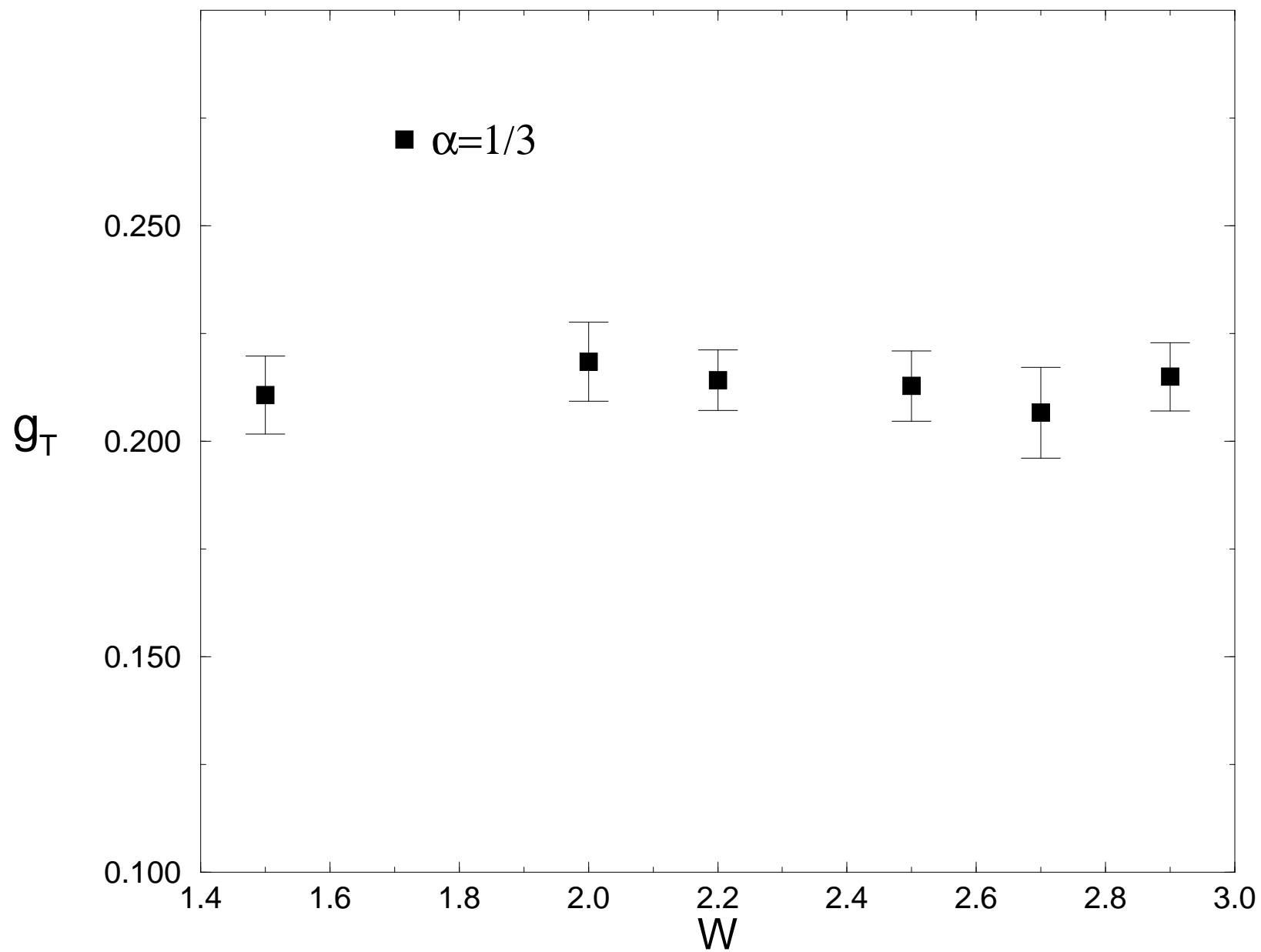


Fig. 11b

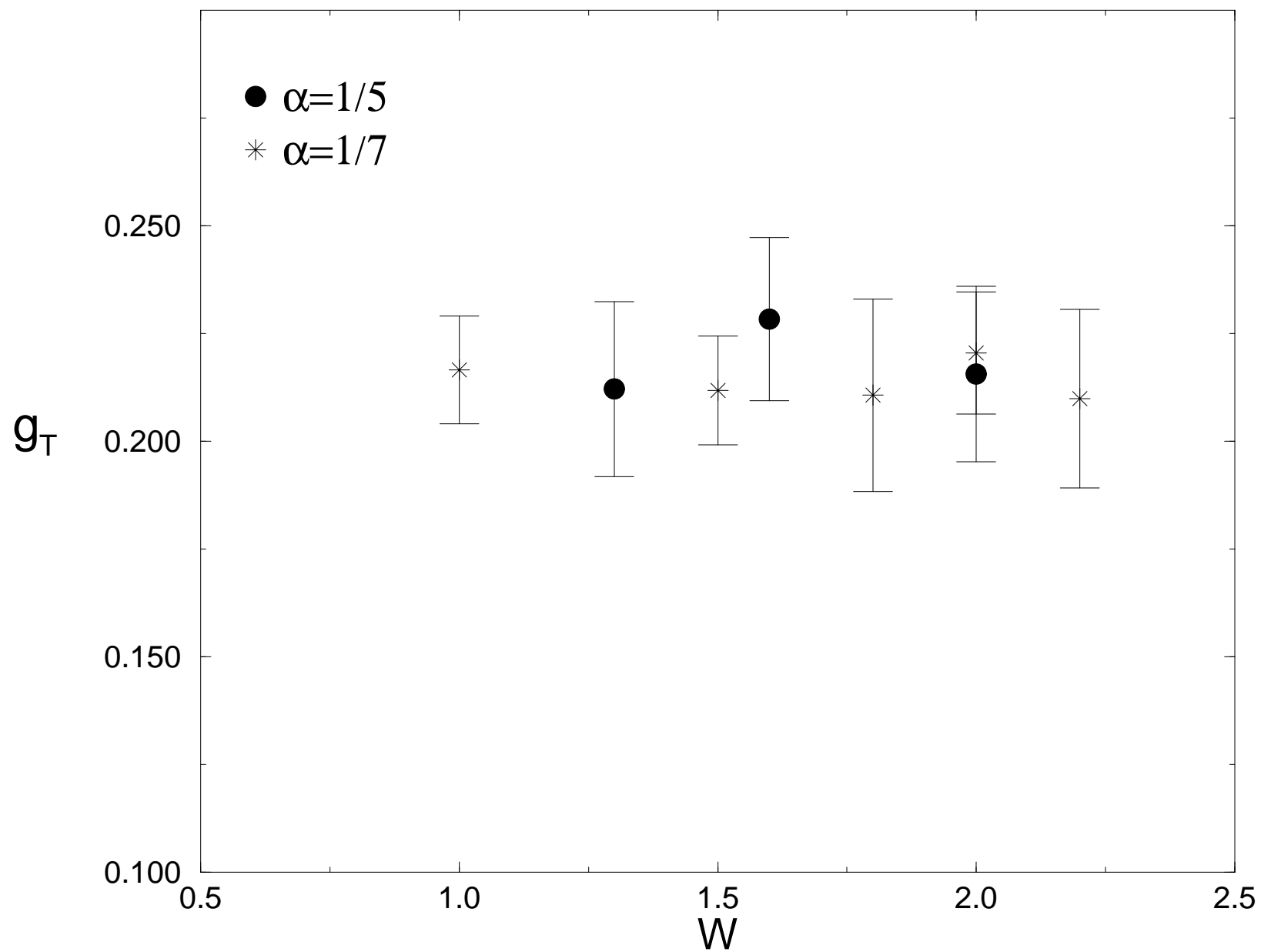




Fig. 12

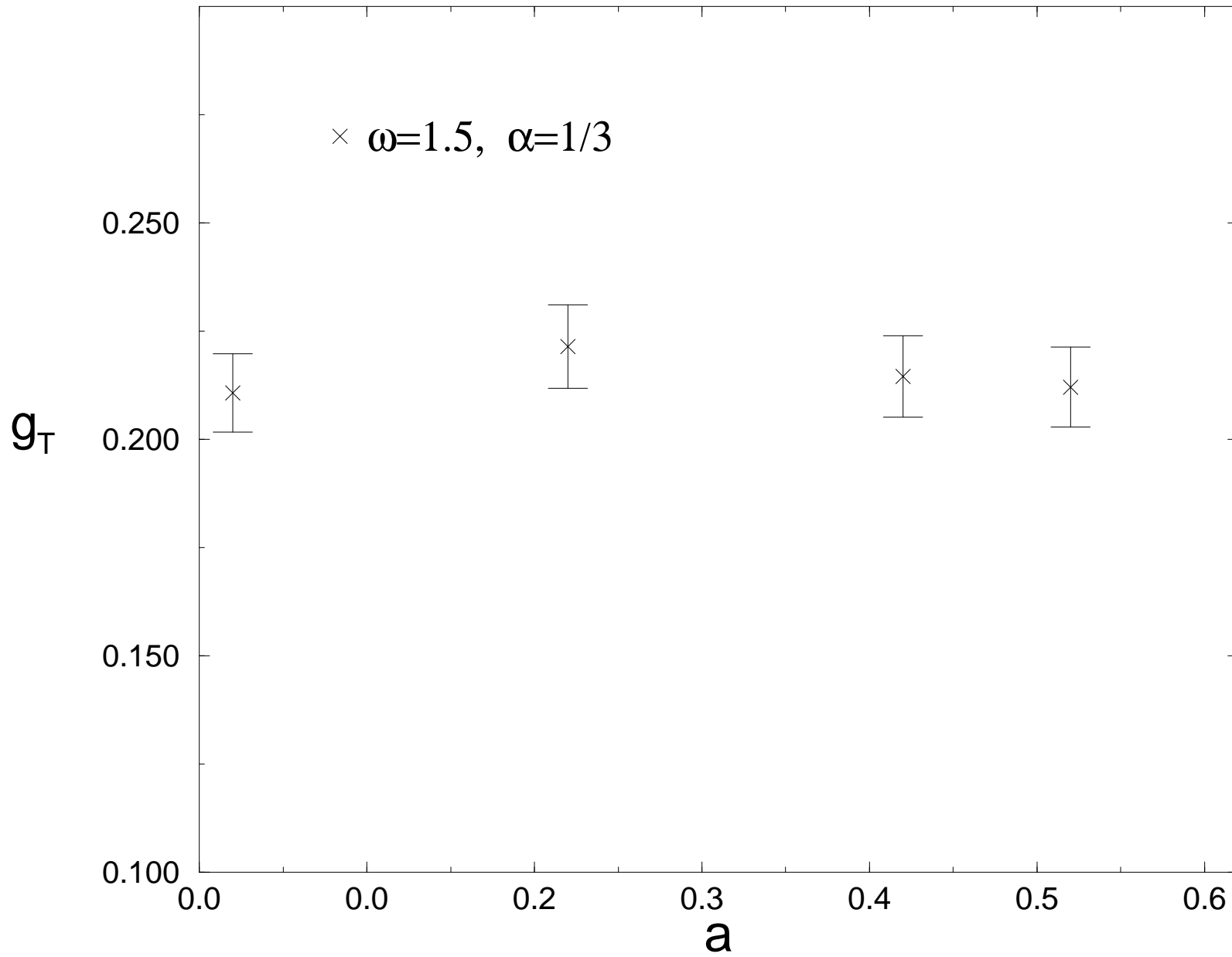


Figure 13

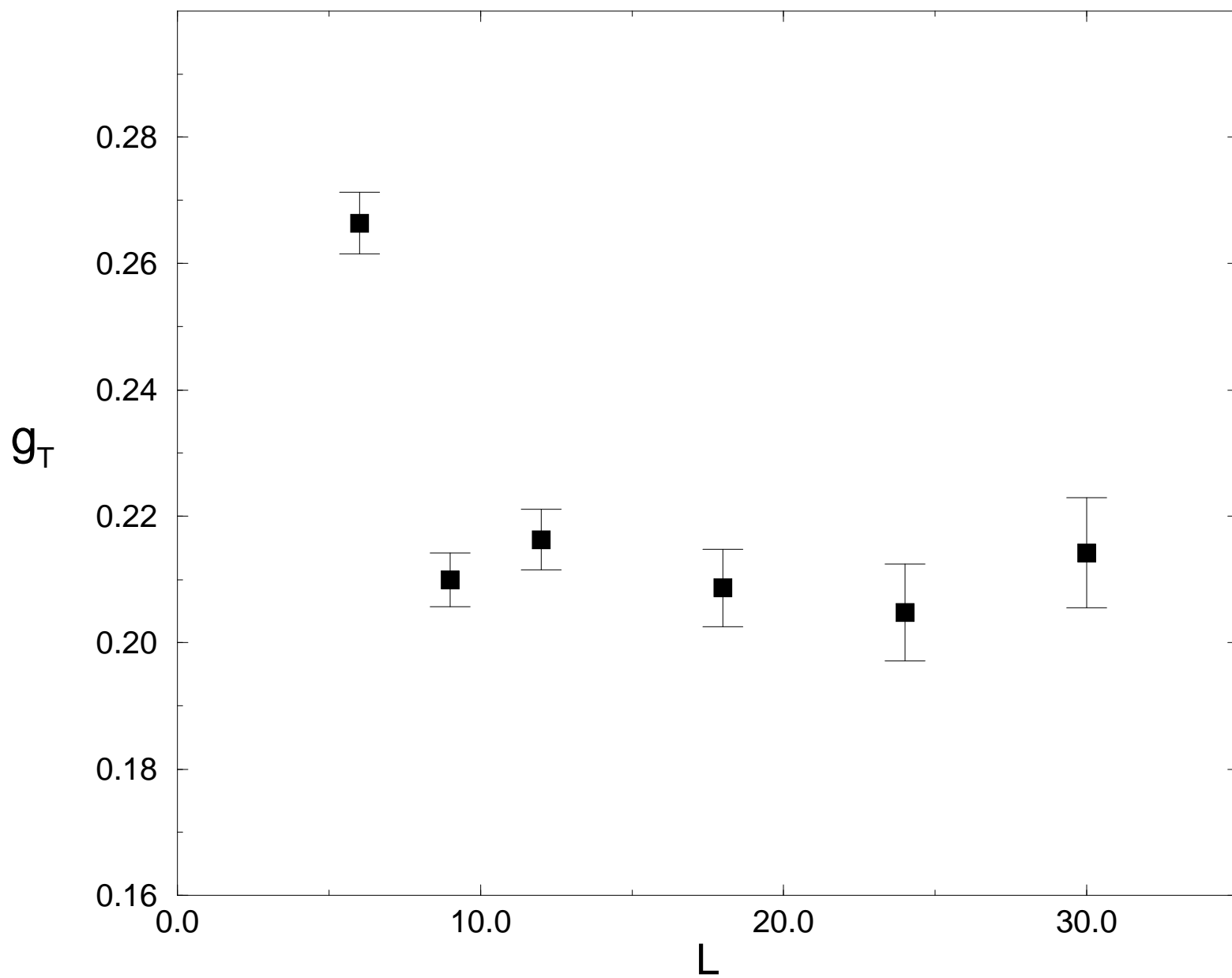


Figure 14

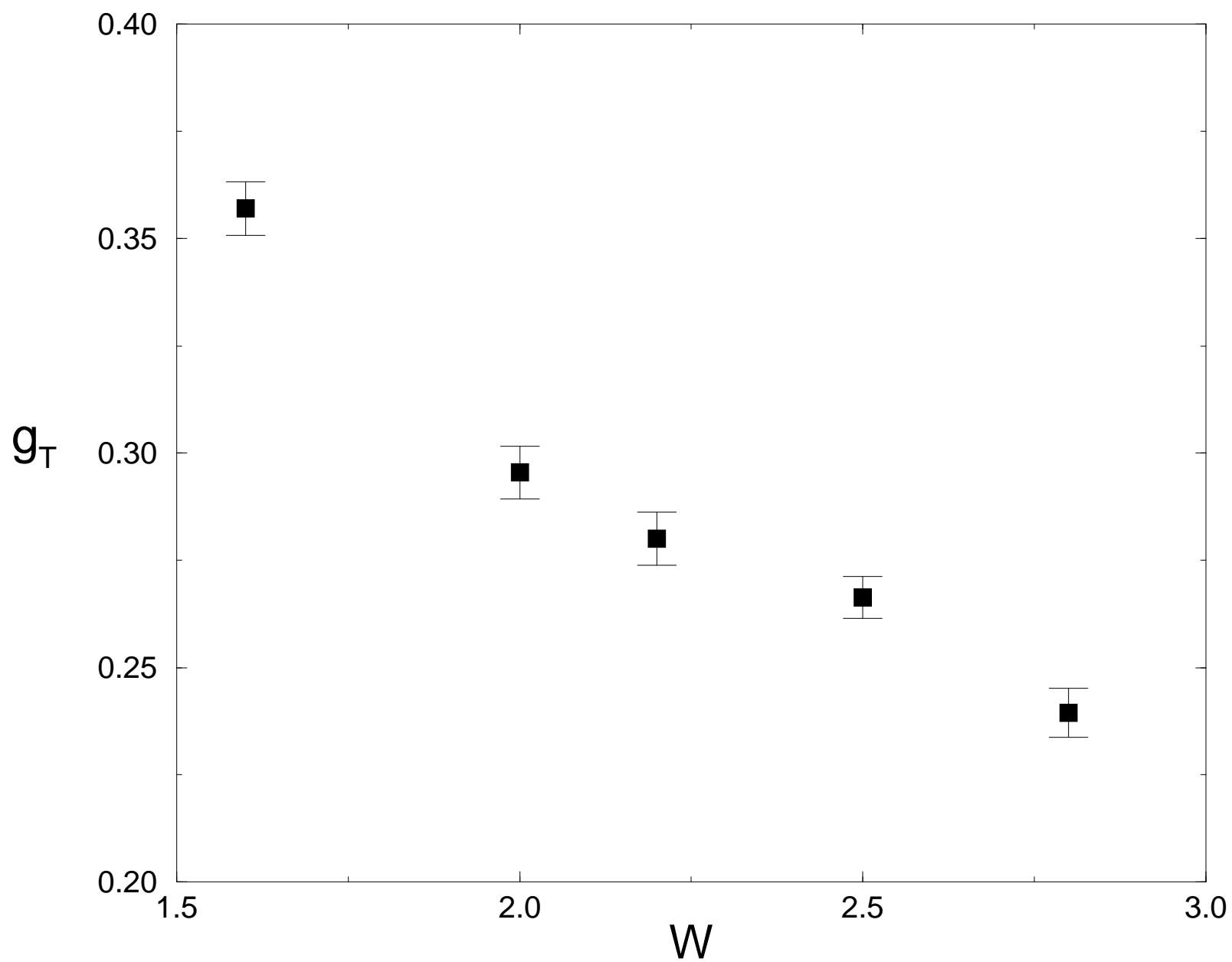


Figure 15

